Supramolecular Multiporphyrin Architecture. Coordination Polymers and Open Networks in Crystals of Tetrakis(4-cyanophenyl)- and Tetrakis(4-nitrophenyl)metalloporphyrin

R. Krishna Kumar, S. Balasubramanian, and Israel Goldberg*

School of Chemistry, Sackler Faculty of Exact Sciences, 69978 Ramat Aviv, Tel Aviv, Israel

Received October 10, 1997

Crystalline solids based on the tetrakis(4-cyanophenyl) and tetrakis(4-nitrophenyl) derivatives of zinc(II)−porphyrin or copper(II)−porphyrin as building blocks have been prepared and structurally analyzed by X-ray diffraction in order to elucidate the characteristic modes of self-assembly of these functionalized moieties and evaluate the utility of such materials in a controlled design of crystalline microporous solids. In suitable crystallization environments, the cyanophenyl derivative was found to form two-dimensional coordination polymers through direct ligation of two of the −C≡N functions on each molecule to the metal centers of two neighboring porphyrins (**1**−**3**). Uniquely structured layered interporphyrin chains and networks with large cavities were observed in most of the other materials (**4**−**9**). The layered organization in the latter is dominated to a large extent by molecular shape and aromaticity of the porphyrin frameworks, while its open nature is sustained by hydrogen-bonding assisted dipolar interactions between the cyanophenyl or nitrophenyl fragments of adjacent metallomacrocyclic units. This gives rise to partly selective cocrystallization of the porphyrin material with suitably sized guest components. The discussion relates also to successful applications of other synthons for engineering polymeric and networked structures of porphyrin-based molecular solids.

Introduction

The ability to control the supramolecular organization of molecular entities by noncovalent interactions is a challenging goal in materials science, on the road to designing new compounds with potentially useful properties for relevant scientific and technological applications.[1] A particular effort is being directed toward the synthesis of functional materials for transport of energy, charge, ions, and molecules.[2] The latter include nanoporous molecular-based solids which reveal structural and functional similarity to the inorganic zeolites. Crystal structure analysis of suitably engineered crystalline materials, combined with the vast crystallographic information available from crystallographic data bases,[3] provides an extremely useful tool for the characterization, systematization, and understanding of the specific forces that direct and stabilize the intermolecular arrangement. It allows the identification of robust supramolecular synthons, which can be particularly useful in the context of crystal engineering of new structures with desired architectures.[4] In a series of earlier publications it was shown that the tetraphenylporphyrin molecules (TPP), with rather poor shape self-complementarity in three dimensions, provide remarkably versatile building blocks for the construction of lattice clathrates.[5] Due to the large size, high symmetry, and rigidity of the molecular units the porphyrin-based host structure was found to be strongly conserved in two dimensions. The TPP clathrates were found to be stabilized primarily by weak dispersive forces. Most of them could be characterized by Strouse et al. in terms of an intercalation-type pattern in which corrugated sheets of stacked porphyrin molecules are interspaced by sheets of the guest species.[5a] The porphyrin sheet structure in the vast majority of these clathrates reveals (a) an offset $\pi-\pi$ stacking of the roughly square-planar molecular units along a direction normal to the porphyrin plane, and (b) $\pi-\pi$ stacking as well as edge-to-face interaction modes between the peripheral phenyl rings within the chain arrangement of the TPP frameworks in a direction parallel to the porphyrin plane.[5,6b,c,e] Lack of any stronger specific interaction between the porphyrin sheets

(1) (a) Philp, D.; Stoddart, J. F. *Angew. Chem., Int. Ed. Engl.* **1996**, *35*, 1154−1196. (b) Lehn, J.-M. *Supramolecular Chemistry*; VCH: Weinheim, 1995. (c) Lehn, J.-M. *Angew. Chem., Int. Ed. Engl.* **1990**, *29*, 1304−1319.

(2) (a) Van Nostrum, C. F.; Nolte, R. J. M. *J. Chem. Soc., Chem. Commun.* **1996**, 2385−2392. (b) Marks, T. J. *Angew. Chem., Int. Ed. Engl.* **1990**, *29*, 857−879.

(3) (a) Allen, F. H.; Kennard, O. *Chem. Design Automation News* **1993**, *8*, 31−37. (b) Allen, F. H.; Kennard, O.; Taylor, R. *Acc. Chem. Res.* **1983**, *16*, 146−153.

(4) (a) Funeriu, D. P.; Lehn, J.-M.; Baum, G.; Fenske, D. *Chem. Eur. J.* **1997**, *3*, 99−104. (b) Shekhar Reddy D.; Ovchinnikov, Yu. T.; Shishkin, O. V.; Struchkov, Yu. T.; Desiraju, G. R. *J. Am. Chem. Soc.* **1996**, *118*, 4085−4089. (c) Shekhar Reddy, D.; Craig, D. C.; Desiraju, G. R. *J. Am. Chem. Soc.* **1996**, *118*, 4090−4093. (d) Thalladi, V. R.; Satish Goud, B.; Hoy, V. J.; Allen, F. H.; Howard, J. A. K.; Desiraju, G. R. *J. Chem. Soc., Chem. Commun.* **1996**, 401−402. (e) Desiraju, G. R. *Angew. Chem., Int. Ed. Engl.* **1995**, *34*, 2311−2327. (f) Su. D.; Wang. X.; Simard, M.; Wuest, J. D. *Supramol. Chem.* **1995**, *6*, 171−178. (g) Etter, M. C. *J. Phys. Chem.* **1991**, *95*, 4601−4610. (h) Etter, M. C. *Acc. Chem. Res.* **1990**, *23*, 120−126.

(5) (a) Byrn, M. P.; Curtis, C. J.; Hsiou, Y.; Khan, S. I.; Sawin, P. A., Tendick, S. K.; Terzis, A.; Strouse, C. E. *J. Am. Chem. Soc.* **1993**, *115*, 9480−9497. (b) Byrn, M. P.; Curtis, C. J.; Goldberg, I., Huang, T.; Hsiou, Y.; Khan, S. I.; Sawin, P. A., Tendick, S. K.; Terzis, A.; Strouse, C. E. *Mol. Cryst. Liq. Cryst.* **1992**, *111*, 135−140. (c) Byrn, M. P.; Curtis, C. J.; Goldberg, I., Hsiou, Y.; Khan, S. I.; Sawin, P. A., Tendick, S. K.; Strouse, C. E. *J. Am. Chem. Soc.* **1991**, *113*, 6549−6557. (d) Byrn, M. P.; Curtis, C. J.; Khan, S. I.; Sawin, P. A.; Tsurumi, R.; Strouse, C. E. *J. Am. Chem. Soc.* **1990**, *112*, 1865−1874. (e) Scheidt, W. R.; Lee, Y. J. *Struct. Bond. (Berlin)* **1987**, *64*, 1−70.

(6) (a) Dance, I.; Scudder, M. *Chem. Eur. J.* **1996**, *2*, 481−486. (b) Hunter, C. A. *Chem. Soc. Rev.* **1994**, 101−108. (c) Hunter, C. A. *Angew. Chem., Int. Ed. Engl.* **1993**, *32*, 1584−1586. (d) Klebe G.; Diederich, F. *Phil. Trans. R. Soc. London* A **1993**, *345*, 37−48. (e) Hunter, C. A.; Sanders, J. K. M. *J. Am. Chem. Soc.* **1990**, *112*, 5525−5534. (f) Jorgensen, W. L.; Severance, D. L. *J. Am. Chem. Soc.* **1990**, *112*, 4768−4774. (g) Burley, S. K.; Petsko, G. A. *J. Am. Chem. Soc.* **1986**, *108*, 7995−8001.

S0020-1669(97)01259-7 CCC: $15.00
Published on Web 01/14/1998

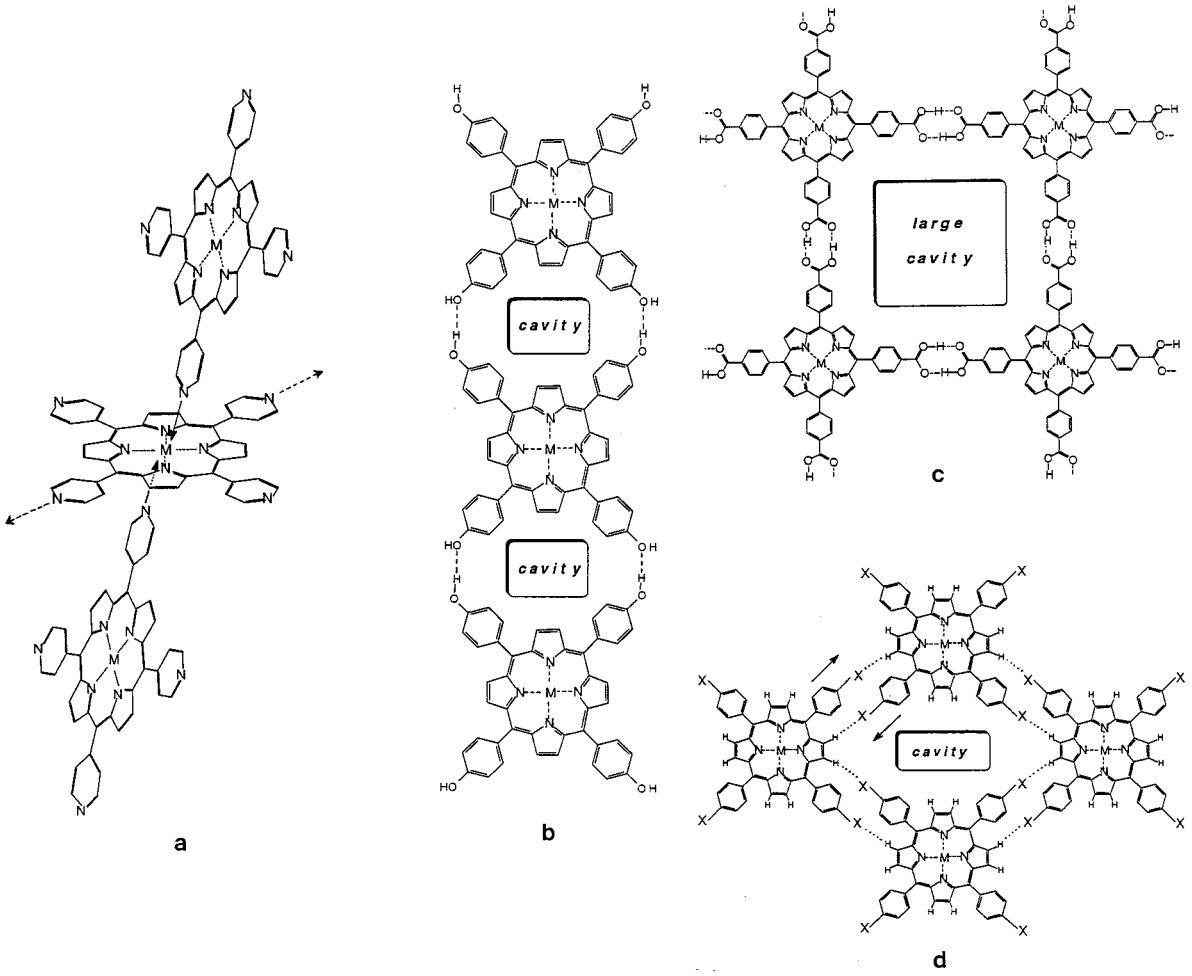

Figure 1. Schematic illustration of multiporphyrin crystalline architectures in (a) coordination polymers of zinc−tetrapyridylporphyrin (the arrows indicate the directions of interporphyrin coordination),[9g] (b) hydrogen-bonding chained polymers of tetrakis(4-hydroxyphenyl)porphyrin,[9f] (c) hydrogen-bonded networks of tetrakis(4-carboxyphenyl)porphyrin,[9b] (d) open layered networks of halogen-substituted derivatives of TPP (X = F, Cl, Br) stabilized by dipolar interactions (dark arrows indicate the antiparallel dipoles, while dotted lines indicate the weak hydrogen-bonding-type attractions).[9a,e,f]

accounts for the high propensity of the TPP host to form lattice intercalates with guests of widely varying shape, size, and composition.

On the basis of on these observations, we have anticipated that a suitable functionalization of the metalloporphyrin framework, on its periphery, with polarized aryl groups by deliberate synthesis can be effectively used to modify the spontaneous buildup of the porphyrin lattice by molecular recognition preferences (geometric as well as functional) of the respective sensor groups.[4] This approach to crystal engineering may lead to more rigidly assembled molecular arrays and to lattice architectures of the porphyrin solids with better defined dimensionality, porosity, and guest selectivity than that in the common porphyrin clathrates.[5] In the first part of this project the structural modifications preserved the approximate square-planar geometry of the metalloporphyrin building blocks, by introducing the same chemical function at the 4-position of all four phenyl groups. This includes addition of substituents capable of axial-ligating to metal ions in the porphyrin center and/or capable of forming specific directional interactions with the neighboring building blocks within the porphyrin plane *via* hydrogen bonds and strong dipolar attractions. The latter should allow directed aggregation of the porphyrin species in the form of porous layered networks, as for example in the case of trimesic acid.[7] The former should enhance formation of oligomers and polymers by axial coordination of one porphyrin species to the metal centers of the neighboring moieties.[8] The effectiveness of this approach to regulating the structural features of the interporphyrin assembly has been demonstrated by us in a series of recent publications.[9] The dominant motifs of supramolecular aggregation obtained in crystals of the differently functionalized porphyrin materials are illustrated in Figure 1. They include planar networks with hollow architectures sustained by either strong hydrogen bonds (in crystals based on

(7) (a) Melendez, R. E.; Krishnamohan Sharma, C. V.; Zaworotko, M. J.; Bauer C.; Rogers, R. D. *Angew. Chem., Int. Ed. Engl.* **1996**, *35*, 2213−2215. (b) Kolotuchin, S. V.; Fenlon, E. E.; Wilson, R. S.; Loweth, C. J.; Zimmerman, S. C. *Angew. Chem., Int. Ed. Engl.* **1995**, *34*, 2654−2656. (c) Herbstein, F. H.; Kapon, M.; Reisner, G. M. *J. Incl. Phenom.* **1987**, *5*, 211−214.

(8) (a) Stibrany, R. T.; Vasudevan, J; Knapp, S.; Potenza, J. A.; Emge, T.; Schugar, H. J. *J. Am. Chem. Soc.* **1996**, *118*, 3980−3981. (b) Kobuke, Y.; Miyaji, H. *J. Am. Chem. Soc.* **1994**, *116*, 4111−4112. (c) Senge, M. O.; Smith K. M. *J. Chem. Soc., Chem. Commun.* **1994**, 923−924. (d) Fleischer, E. B.; Shachter, A. M. *Inorg. Chem.* **1991**, *30*, 3763−3769. (e) Shachter, A. M.; Fleischer, E. B.; Haltiwanger, R. C. *J. Chem. Soc., Chem. Commun.* **1988**, 960−961.

(9) (a) Dastidar, P.; Krupitsky, H.; Stein, Z.; Goldberg, I. *J. Incl. Phenom.* **1996**, *24*, 241−262. (b) Dastidar, P.; Stein, Z.; Goldberg, I.; Strouse, C. E. *Supramol. Chem.* **1996**, *7*, 257−270. (c) Dastidar, P.; Goldberg, I. *Acta Crystallogr., Sect. C* **1996**, *52*, 1976−1980. (d) Goldberg, I. *Mol. Cryst. Liq. Cryst.* **1996**, *278*, 57−64. (e) Krupitsky, H.; Stein, Z.; Goldberg, I. *J. Incl. Phenom.* **1995**, *20*, 211−232. (f) Goldberg, I.; Krupitsky, H.; Stein, Z.; Hsiou, Y.; Strouse, C. E. *Supramol. Chem.* **1995**, *4*, 203−221. (g) Krupitsky, H.; Stein, Z.; Goldberg, I.; Strouse, C. E. *J. Incl. Phenom.* **1994**, *18*, 177−192.

4−hydroxyphenyl or 4-carboxyphenyl derivatives) or effective H-bond-assisted dipolar attractions [in materials based on the tetrakis(4-halogenophenyl)porphyrin building blocks], as well as coordination polymers of varying dimensionality based on the tetrapyridylporphyrin unit and maintained by direct metal-to-ligand interactions.[10] The layered aggregates, with cavity dimensions affected by the type of the interacting functional groups, give rise to the incorporation of suitably shaped guest components into the crystal. The selectivity features of these inclusion phenomena should be considerably more pronounced in solids based on the functionalized building blocks[9] than in the previously studied "porphyrin sponges" (crystalline clathrates formed by unsubstituted TPP molecules).[5]

In this work we extend our evaluation to materials based on the metallated tetrakis(4-cyanophenyl)porphyrin [TCNPP] and tetrakis(4-nitrophenyl)porphyrin [TNO_2PP] building blocks. The linear −CN function is strongly polar, its nitrogen site is a good proton acceptor in hydrogen bonds, and it is also an excellent ligand to transition metal atoms.[11] Moreover, a review of recent literature reveals that a dimeric aggregate of CN-substituted aromatic fragment is a very robust supramolecular synthon in crystals of organic entities.[3,4] This provides a strong motivation for the use of the CN-functionalized porphyrin entities to study the regulating effect of this function on supramolecular organization of these metallomacrocycles in the solid state. Several different modes of intermolecular aggregation appear plausible in the present case due to the multifunctional nature of the −CN substituent (see above). It has been assumed, therefore, that the resulting structure type can be affected to a major extent by the crystallization environment. Similar considerations apply to the polar $-NO_2$ substituent, which also has coordination capacity to transition metals[8c] and can act as a proton acceptor in hydrogen bonds (the multiple H-binding sites of this function allow in principle to form networks of higher dimensionality). The October 1996 version of the Cambridge Crystallographic Database[3] contains only a single entry of structural characterization of the TCNPP derivative[10b] and none relating to the TNO_2-PP moiety. A comprehensive evaluation of the structural patterns and supramolecular interactions in a series of newly prepared crystalline forms of the title compounds is thus presented below. This includes inclusion solids of (a) zinc−TCNPP with 2 mol of nitrobenzene (**1**, $C_{48}H_{24}N_8Zn\cdot 2C_6H_5NO_2$), 1 mol of chloroform (**2**, $C_{48}H_{24}N_8Zn\cdot CHCl_3$), 1 mol of anisole (**3**, $C_{48}H_{24}N_8Zn\cdot C_7H_8O$), 2 mol of ethyl benzoate (**5**, $C_{48}H_{24}N_8Zn\cdot 2C_9H_{10}O_2$), 2.5 mol of anisole (**6**, $C_{48}H_{24}N_8Zn\cdot 2.5C_7H_8O$), 3 mol of guaiacol (**7**, $C_{48}H_{24}N_8Zn\cdot 3C_7H_8O_2$), 1 mol of chloroform and of benzene (**9**, $C_{48}H_{24}N_8Zn\cdot CHCl_3\cdot C_6H_6$); (b) of zinc−$TNO_2PP$ with 3 mol of eugenol (**8**, $C_{44}H_{24}N_8O_8Zn\cdot 3C_{10}H_{12}O_2$); and (c) of copper−TCNPP with 2 mol of chlorofom (**4**, $C_{48}H_{24}N_8Cu\cdot 2CHCl_3$) and 2 mol of nitrobenzene (**10**, $C_{48}H_{24}N_8Cu\cdot 2C_6H_5NO_2$). In view of the versatile engagement of TCNPP in intermolecular interactions, correlations of the observed motifs with those previously found for tetraarylporphyrin materials functionalized with other groups are particularly instructive.

Experimental Section

Preparative Procedures. The starting materials, *p*-cyanobenzaldehyde, *p*-nitrobenzaldehyde, *p*-chloranil, and pyrrole, were obtained from Aldrich. ^{1}H-NMR spectra were obtained at 200 MHz (Bruker) instrument. IR were recorded on a Nicolet 205 FTIR spectrometer. FAB mass spectral analyses were performed on a VG Autospec, M250 Q mass spectrometer; elemental analysis for C, H, and N was performed on a PE Elemental Analyzer 2400 Series II. TGA and DTA measurements were performed using TA Instruments module 910 and system controller 2100. The title compounds were prepared by the following procedures adapted from the literature.[12a,b]

***meso*-Tetrakis(4-cyanophenyl)porphyrin.** Freshly distilled pyrrole (0.42 mL, 0.403 g, 6 mmol) was added to *p*-cyanobenzaldehyde (0.78 g, 6 mmol) dissolved in 400 mL of dry CH_2Cl_2. This mixture was then treated first with 0.16 mL of a 2.5 M solution of BF_3 etherate in CH_2Cl_2 (0.398 mmol) under continuous stirring for 2 h, and subsequently with *p*-chloranil (1.11 g, 4.5 mmol) upon heating for 1 h at 45 °C. The solvent was removed from the reaction vessel, and the crude product was column chromatographed on silica using $CHCl_3$ as eluent to yield 0.396 g (37%) of pure *meso*-tetrakis(4-cyanophenyl)porphyrin $C_{48}H_{26}N_8$, 714.2 calculated mass (M), 715 (MH^+). ^{1}H-NMR ($CDCl_3$) δ: −2.92 (s, 2H, NH), 8.14, 8.36 (d,d, J = 8.0 Hz, 16H, C_6H_4), 8.82 (s, 8H, β-pyrrole). IR (neat, $CHCl_3$): 2230 (CN) cm^{-1}. The isolated product (0.200 g, 0.28 mmol) dissolved in 20 mL of DMF was heated to boiling, and 0.100 g (0.45 mmol) of zinc acetate, $Zn(OAc)_2\cdot 2H_2O$, or a corresponding Cu(II) salt was added. After cooling, the resulting mixture was diluted with water (20 mL), yielding a dark precipitate. The product was filtered, air-dried, and further purified by column chromatography to yield the metallated porphyrin compound (mp > 350 °C).

***meso*-Tetrakis(4-nitrophenyl)porphyrin.** *p*-Nitrobenzaldehyde (5.5 g, 36.42 mmol) dissolved in 150 mL of propionic acid was treated under reflux conditions, first with acetic anhydride (6 mL, 6.43 g, 63.59 mmol) and then with freshly distilled pyrrole (2.5 mL, 2.42 g, 36.16 mmol) dissolved in 5 mL of propionic acid. After 24 h the resulting solid was collected by filtration and treated with 40 mL of pyridine. Additional filtration of the precipitate, followed by a thorough rinsing with acetone and air-drying yielded 1.8 g of the solid product: *meso*-tetrakis(4-nitrophenyl)porphyrin. $C_{44}H_{26}N_8O_8$, 794.7 calculated mass (M), 795 (MH^+). ^{1}H-NMR ($CDCl_3$) δ: −2.84 (s, 2H, NH), 8.39, 8.67 (d,d, J = 8.0 Hz, 16H, C_6H_4), 8.81 (s, 8H, β-pyrrole). IR (neat, $CHCl_3$): 1500, 1330 (NO_2) cm^{-1}. The isolated porphyrin was directly used for metallation (as described above) without any further purification. Metallation reactions of the two porphyrin derivatives were carried out with about 90% yields.

Crystallization of the Composite Materials. Single crystals of the composite materials were obtained by recrystallization of the metallated porphyrin derivatives, under controlled conditions, either directly from saturated solutions of the respective guest solvents, or from its solution in chloroform (used initially for dissolving the porphyrin) to which was added the corresponding guest component. In the latter case, a 1:1 chloroform-to-guest component ratio was maintained in the crystallization environment. In addition to the crystallographic determinations based on diffraction data (see below), the composition of the crystalline materials obtained in sufficient quantity was confirmed also by elemental analysis (for C, H, and N) and by assessment of weight loss (due to guest/solvent evaporation) in TGA measurements. Calcd for **1**: C, 70.35; H, 3.34; N, 13.67. Found: C, 69.92; H, 3.40; N, 13.35. TGA shows loss of 2 mol of nitrobenzene within the range 90−115 °C. Calcd for **6**: C, 74.88; H, 4.05; N, 11.27. Found: C, 73.82; H, 4.29; N, 10.50. Cald for **7**: C, 72.03; H, 4.20; N, 9.74. Found: C, 72.01; H, 4.40; N, 9.86. TGA shows loss of 3 mol of

(10) Coordination polymerization of similarly functionalized tetraphenylporphyrin species, but through transition metal bridges, has been reported in the following: (a) Drain, C. M.; Lehn, J.-M. *J. Chem. Soc., Chem. Commun.* **1994**, 2313−2315. (b) Abrahams, B. F.; Hoskins, B. F.; Michail, D. M.; Robson, R. *Nature* **1994**, *369*, 727−729. (c) Abrahams, B. F.; Hoskins, B. F.; Robson, R. *J. Am. Chem. Soc.* **1991**, *113*, 3606−3607.

(11) (a) The C−H···N hydrogen bonding in HCN was characterized a long time ago by Dulmage, W. J.; Lipscomb, W. N. *Acta Crystallogr.* **1951**, *4*, 330−334. For more recent examples of interactions involving −CN see: (b) Gardner, G. B.; Venkataraman, D.; Moore, J. S.; Lee, S. *Nature* **1995**, *374*, 792−795. (c) Iwamoto, T. *Inclusion Compounds*; Oxford University Press: Oxford, 1991; Vol. 5, pp 177−212.

(12) (a) Lindsey, J. S.; Schreiman, I. C.; Hsu, H. C.; Kearney, P. C.; Marquerettez, A. M. *J. Org. Chem.* **1987**, *52*, 827−836. (b) Bettleheim, A.; White, B. A.; Raybuck, S. A.; Murray, R. W. *Inorg. Chem.* **1987**, *26*, 1010.

Table 1. Crystallographic Data for Compounds **1**−**10**

compound	**1**	**2**	**3**	**4**	**5**	**6**	**7**	**8**	**9**	**10**
FW[a]	1024.4	897.5	886.3	1015.0	1078.5	1048.5	1150.5	1350.7	975.6	1022.5
space group	$P2_1/n$	$C2/c$	$P\bar{1}$	$P\bar{1}$	$P\bar{1}$	$P\bar{1}$	$P\bar{1}$	$P\bar{1}$	$P2_1/c$	$P2_1/c$
Z	2	4	2	2	2	1	1	2	4	2
a, Å	12.953(3)	25.368(4)	8.841(6)	9.656(2)	11.578(2)	8.889(2)	8.870(2)	12.996(3)	9.570(4)	13.706(3)
b, Å	9.061(2)	8.089(2)	11.818(4)	15.111(4)	13.579(2)	11.607(2)	12.406(3)	16.404(5)	30.037(7)	24.138(6)
c, Å	21.131(6)	22.425(5)	22.079(5)	17.261(3)	17.387(5)	13.647(3)	12.985(2)	16.673(4)	16.099(6)	7.624(3)
α, deg	90.0	90.0	87.05(2)	115.36(2)	85.17(2)	94.74(1)	85.89(2)	110.76(2)	90.0	90.0
β, deg	102.69(2)	111.12(1)	89.37(5)	95.51(1)	82.09(2)	96.40(2)	86.91(2)	99.57(2)	97.71(3)	105.78(3)
γ, deg	90.0	90.0	69.62(5)	95.10(2)	87.79(1)	90.27(2)	87.65(2)	91.19(2)	90.0	90.0
V, Å^3	2419.5	4292.5	2159.6	2241.6	2696.9	1394.3	1422.1	3265.2	4585.9	2427.2
D_{calcd}, g cm^{-3}	1.41	1.39	1.36	1.50	1.33	1.25	1.34	1.37	1.41	1.40
F(000)	1052	1824	912	1026	1116	543	596	1404	1992	1050
μ, mm^{-1}	5.7	8.0	6.2	8.9	5.1	4.9	4.9	4.51	7.6	5.1
2θ limits, deg	50	50	42	46	42	50	50	42	42	46
N (unique) > 0	3876	2457	4083	5612	4926	4596	4737	5685	4118	2658
N [$I < 2\sigma(I)$]	3071	1838	3147	4122	3244	3833	4042	3559	2705	1720
R [$I < 2\sigma(I)$]	0.044	0.134[c]	0.108	0.091[d]	0.067	0.102[f]	0.112[g]	0.078	0.102[h]	0.084
R' [$I < 2\sigma(I)$][b]	−	0.065[c]	−	0.061[e]	−	0.054[f]	0.059[g]	−	0.067[i]	−

[a] Formula weights refer to the following compositions: **1**, $C_{48}H_{24}N_8Zn\cdot 2C_6H_5NO_2$; **2**, $C_{48}H_{24}N_8Zn\cdot CHCl_3$; **3**, $C_{48}H_{24}N_8Zn\cdot C_7H_8O$; **4**, $C_{48}H_{24}N_8Cu\cdot 2CHCl_3$; **5**, $C_{48}H_{24}N_8Zn\cdot 2C_9H_{10}O_2$; **6**, $C_{48}H_{24}N_8Zn\cdot 2.5C_7H_8O$; **7**, $C_{48}H_{24}N_8Zn\cdot 3C_7H_8O_2$; **8**, $C_{44}H_{24}N_8O_8Zn\cdot 3C_{10}H_{12}O_2$; **9**, $C_{48}H_{24}N_8Zn\cdot CHCl_3\cdot C_6H_6$; **10**, $C_{48}H_{24}N_8Cu\cdot 2C_6H_5NO_2$. [b] Calculated for ordered fragments of the structure, without the disordered solvent, following the Squeeze/Bypass procedure (see text).[14] [c] The disordered molecule of chloroform was not included in the structure factor calculations. [d] Including the two located, but partly disordered, molecules of chloroform. [e] Excluding the chloroform species. [f] Excluding the noncoordinated disordered anisole species. [g] Excluding the noncoordinated disordered guaiacol species. [h] Including disordered molecules of the benzene and chloroform solvents. [i] Excluding the solvents.

guaiacol at two stages: 19.8% and 8.9% weight loss within 101−108 and 161−168 °C, respectively. Pure crystalline material of the other composite compounds was obtained on a 1 mg scale only, which did not allow reliable determination of the guest/solvent content in the corresponding porphyrin crystals by standard methods.

X-ray Diffraction Studies. All diffraction data were collected at room temperature (ca. 298 K) on an Enraf-Nonius CAD4 diffractometer using graphite-monochromated Mo Kα ($\lambda = 0.7107$ Å) radiation and $\omega-2\theta$ scans. Some crystals were coated with epoxy resin to prevent loss of the guest component. Full details of the routinely applied experimental procedures are reported in previous publications of this series.[9] All structures were solved by direct methods using SHELXS-86[13a] and then refined by least squares using the SHELXL-93 program.[13b] The crystal data and pertinent details of the experimental parameters are summarized in Table 1. Some difficulties were experienced in the refinement procedures, similar to those typically observed in related studies of composite porphyrin structures.[5,9] They were mostly due to apparent disorder of the smaller component incorporated into the crystal but not coordinated to the porphyrin lattice (a phenomenon quite common in the porphyrin clathrates), and failure to define a satisfactory structural model for this disorder. In order to confirm the correctness of the interporphyrin organization and interaction scheme, the refinement calculations of the ordered fragments only were repeated in such cases by using the "Squeeze/Bypass" technique in which the overall contribution of disordered solvent (located mostly in channel-type voids of the lattice) to the diffraction pattern is substracted from the observed data.[14] This approach was applied to structures **2**, **4**, **6**, **7**, and **9**, resulting in good convergence of the refinement at reasonably low R values (Table 1). In **2**, the positions of the chloroform species trapped between layers of the porphyrin coordination polymers could not be located. The residual electron density in the interporphyrin voids accommodating the solvent within the unit cell was assessed by "Squeeze" to be 277e, only slightly larger than the calculated value of 232e for four molecules of chloroform. In **4**, the two-chloroform species, although partly disordered, could be located in the difference-Fourier map. However, conventional refinement of the entire structure converged poorly at $R = 0.091$; after the electron density was "squeezed out" at the chloroform sites (assesed as 235 electrons in the unit cell), it went down to $R = 0.061$. Similarly in **9**, which contains partly disordered molecules of chloroform and benzene, the R value decreased from 0.102 (for the whole structure including a 2-fold disorder model for the chloroform) to 0.067 (for the porphyrin lattice only). In the latter calculations, the residual electron count in the interporphyrin voids amounts to 403.6, in good agreement with the stoichiometric composition (four molecules of benzene and four molecules of chloroform in the unit cell, totaling 400e). Compounds **6** and **7** consist of well-defined six-coordinate metalloporphyrin entities with either anisole or guaiacol, respectively, occupying the axial coordination sites of the metal center. Moreover, the two solids appeared to contain additional moieties of heavily disordered solvent, positions of which could not be reliably located. Application of the "squeeze" technique to the latter allowed smooth convergence of the refinement down to R values of 0.054 (**6**) and 0.059 (**7**), and electron counts within the interporphyrins voids of 38e (**6**, corresponding to slightly more than 0.5 molecule of anisole) and of 76e (**7**, corresponding roughly to one molecule of guaiacol). The residual electron density data which represent in the individual structures the disordered solvent provide (particularly in view of their reasonably good agreement with the results of elemental and TGA analyses for compounds **6** and **7**; see above) supporting indications of the stoichiometric compositions assumed in the crystallographically refined structural models in the relevant compounds. A somewhat poor R value, associated with the appearance of two high residual electron density peaks of ∼1.2 e Å^{-3} in the vicinity of the metal atom, was obtained in structure **3** and could not be explained by absorption effects. It should be attributed to poor quality of, and presence of impurities in, the analyzed crystals of this material, all of which were characterized by large mosaic spread. The partial structural disorder of the eugenol components in **8** (particularly of the $-CH_2CH_3$ tails) did not allow a good convergence of the refinement procedure either (final $R = 0.078$). In all cases, the hydrogen atoms were placed in calculated positions and added as fixed contributions to the structure factors.

Results

TCNPP and TNO_2PP were prepared and metallated by Zn or Cu, and crystals suitable for X-ray diffraction were obtained under varying conditions from different crystallization environ-

(13) (a) Sheldrick, G. M.; SHELXS-86. In *Crystallographic Computing 3*; Sheldrick, G. M., Kruger, C., Goddard, R., Eds.; Oxford University Press: Oxford, 1985, pp 175−189; *Acta Crystallogr., Sect. A* **1990**, *46*, 467−473. (b) Sheldrick, G. M.; *SHELXL-93. Program for Refinement of Crystal Structures from Diffraction Data*; University of Göttingen: Germany, 1993.

(14) (a) Van der Sluis, P.; Spek, A. L. *Acta Crystallogr., Sect. A* **1990**, *46*, 194−201. (b) Spek, A. L. *Acta Crystallogr., Sect. A* **1990**, *46*, C34.

Table 2. Coordination Parameters of the Metal Center in the Various Materials

compound	M−N(porphyrin) bond length rate (Å)	metal coordination number and type of axial ligands (Å)	Zn−axial ligand distances (Å)	shape of the metalloporphyrin core
1	2.044(2)−2.051(2)	6, C≡N	2.726(3)	planar
2	2.042(6)−2.049(5)	6, C≡N	2.80 (1)	planar
3[a]	2.04(1)−2.07(1)	6, C≡N	2.70 (1), 2.74 (2)	planar
4[b]	1.978(4)−1.993(4)	4	−	saddle
5	2.039(6)−2.064(6)	5, C═O	2.224(6)	saddle
6	2.028(2)−2.044(3)	6, aryl π-ring	3.37[c]	planar
7	2.034(2)−2.047(2)	6, OH	2.581(3)	planar
8[a]	2.034(6)−2.057(9)	6, OH	2.519(8), 2.601(8)	planar
9	2.007(7)−2.047(7)	4	−	saddle
10[b]	1.997(7)−2.009(9)	4	−	planar

[a] In compounds **3** and **8** there are two independent porphyrin moieties in the asymmetric unit. [b] The metal center consists of Cu(II) in **4** and **10** and of Zn(II) in the other structures. [c] Average distance between the benzene ring of anisole and the N_4Zn plane of the porphyrin core.

Table 3. Parameters of Interporphyrin Interaction in Compounds **4**−**10**

compound	interporphyrin chain direction in the crystal	M−M distances along the chain (Å)	hydrogen bonds[b] C≡N···HC or NO_2···HC (Å)	hydrogen bonds[b] N···H−C or O···H−C (deg)	distances between the interacting aryl groups[a] (Å)	displacement between adjacent chains in the layered motif (Å)	average interlayer spacing (Å)
4	$a + b$ and c	17.19, 17.26	3.41−3.59 [2.42−2.72]	137−151	3.92[c]	15.52 and 15.58	3.78
5	$a - b$ and c	17.39, 17.50	3.50−3.68 [2.44−2.66]	158−167	3.74[c]	17.38 and 17.50	4.42
6	$b + c$	17.17	3.45 [2.41]	161	3.58	19.88	4.09
7	$b - c$	17.30	3.51 [2.45]	167	3.55	20.06	4.10
8[a]	c	16.67	3.44−3.50 [2.44−2.45]	152−164	3.46	23.34	4.19
9	$a + c$	17.59	3.79−4.05 [2.73−3.20]	135−164	3.91[c]	15.02	4.34
10	$a + 2c$	17.51	3.67 [2.62]	163	3.63	−	−

[a] In **8** interporphyrin interaction is through the $ArNO_2$ side groups; in all other compounds it is through the ArCN substituents. [b] Values in square brackets refer to H···N or H···O (in **8**) distances. [c] In **4**, **5**, and **9** the interacting groups are not parallel to each other. In these structures the average interplanar distances between the overlapping functions, given for **6**−**8** and **10**, are replaced by a distance between the main axes of the interacting ArCN groups.

ments, containing either "inert" solvents or ligands with axial coordination potential to the metal center or both. Correspondingly, four-, five-, and six-coordinate metalloporphyrin structures were obtained. The resulting materials represent several characteristic types of the interporphyrin organization, the preference of one type over another depending on solvating and ligating properties of the guest/solvate component. Several different materials based on the tetrakis(4-nitrophenyl) derivative could be obtained, but only one of these provided single crystals suitable for X-ray studies. Selected structural details related to the porphyrin conformation, metal−ligand binding and interporphyrin coordination are given in Tables 2 and 3; the remaining crystallographic data are included in the Supporting Information.

Coordination Polymers. Crystallizations of the zinc-metallated TCNPP from pure chloroform, as well as from most solvent mixtures containing chloroform, led to the self-assembly of two-dimensional coordination polymers of the porphyrin moieties. The interporphyrin polymeric architecture in the corresponding solids is propagated by metal−ligand interaction, each monomeric unit being linked to four neighboring porphyrin units. It utilizes two *trans*-related cyano substituents to ligate with the metal center of two adjacent porphyrins along one axis, while the metal ion at the center of each TCNPP binds two cyano functions of other monomeric units approaching from both sides of the molecular framework as axial ligands. Adjacent porphyrin species which link to each other are at different orientations to facilitate coordination, the dihedral angle between their mean planes being near 120°. This layered polymeric pattern is illustrated in Figure 2a. It occurs with very little variation in crystals **1**, **2**, and **3**, irrespective of the differences in their composition and space symmetry. Thus, the translational symmetry within these layers is characterized by 9.1 Å (**1** and **2**) or 8.8 Å (**3**) displacement of the porphyrin building blocks in one direction and by 22.2 Å (**1**, along the $a + c$ axis of the unit cell), 22.4 Å (**2**, along c) or 22.1 Å (**3**, along c) displacement in the other direction. Moreover, the coordination distances and approach angles of the ligating linear −CN groups to the porphyrin metal center are similar in the three structures ranging within 2.7−2.8 Å and 123−129°, respectively (Table 2).

The corrugated surface of the polymeric layer, lined with those cyanophenyl arms of the porphyrin constituents which do not ligate to the metal ions of adjacent units, prevents dense packing and leads to the intercalation of the solvate/guest species between these layers. Figure 2b illustrates the crystal structure **1**, crystallized from a mixture of chloroform and nitrobenzene, in which molecules of the latter are incorporated within the interlayer voids. The polymeric layers are aligned parallel to the $(\bar{1}01)$ lattice plane and to the b axis of the unit cell with an interlayer distance (center-to-center) of 12.0 Å. The nitrobenzene species are located in channels centered at $x = 0$, $z = 0$, and $x = 0.5$, $z = 0.5$, and they lie nearly perpendicular to the channel axis. Crystals obtained from pure chloroform (**2**) exhibit very similar interporphyrin organization, but the polymeric sheets are aligned parallel to the (100) lattice planes; the interlayer distance is 11.8 Å. The presence of the chloroform molecules in the interlayer voids is evident from the accumulated

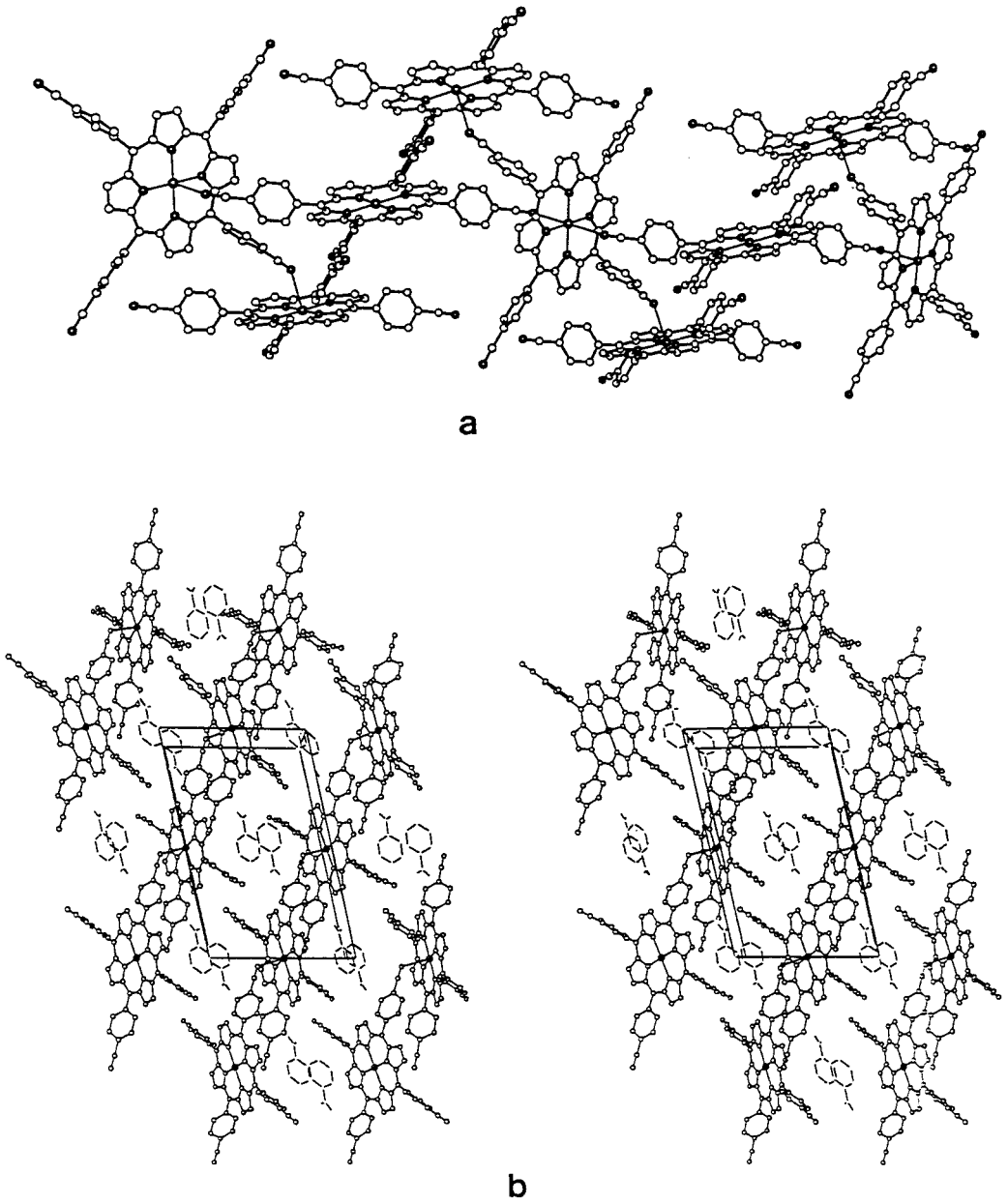

Figure 2. Coordination polymers of zinc−TCNPP. (a) Illustration of the two-dimensional polymeric array in **1** (nearly identical polymeric self-assembly was found in **2** and **3**. (b) Stereoview of the crystal structure of **1** down the *b* axis of the unit cell (*a* is horizontal), showing intercalation of nitrobenzene molecules within channels between the polymeric layers in the crystal lattice.

count of the residual electron density (see Experimental Section). In these two structures adjacent porphyrin frameworks are related by the glide-plane/screw-axis symmetry. A nearly identical supramolecular organization is maintained in **3**, where the coordination polymers extend parallel to the (010) lattice planes with an interlayer spacing of 11.8 Å (Figure 3). This compound forms a triclinic lattice but with two differently oriented porphyrin entities in the asymmetric unit (to facilitate the interporphyrin coordination). In this case, the porphyrin material was crystallized from a mixture of chloroform and anisole, but only the latter was extracted from the solvent mixture into the crystal lattice to fill the interlayer voids. The selective solvent incorporation of nitrobenzene and of anisol from their corresponding mixtures with chloroform should be attributed mainly to the different shapes of these three molecules. The nitrobenzene and anisol components are bulkier than chloroform, fit better the size of the interporphyrin voids, and thus lead to the formation of cocrystals with a somewhat higher stability. It appears also that the relatively high polarity of nitrobenzene and the tendency of these species to pair in antiparallel orientations affect the composition of the porphyrin−solvate cocrystals which form (the stoichiometry is 1:2 with nitrobenzene in **1**, but only 1:1 with anisole in **3**).

Open Two-Dimensional Networks. Structures **4** and **5** represent another interesting pattern of interporphyrin organization. It can be obtained when the self-coordination referred to above is made less feasible by (a) introducing into the solvent mixture polar components which can serve as preferred axial ligands to the metal ion or (b) exchanging the divalent zinc in the porphyrin center to Cu(II) which has a lesser affinity for axial coordination (square-planar coordination around divalent copper is most common). Indeed, crystallization of Cu(II)−TCNPP from pure chloroform leads (in **4**) to a coplanar arrangement of the porphyrin units in which the Cu ion is four-coordinate, as shown in Figure 4a. The dominant structural motif consists of linear chains of the porphyrin species. This

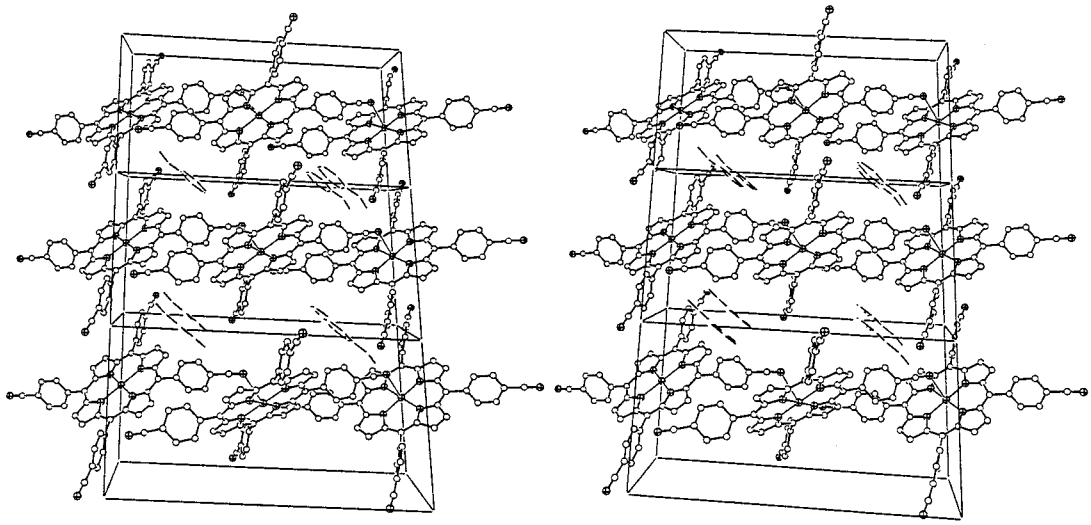

Figure 3. Stereoview of the crystal structure of **3** approximately down the *a*-axis (*c* is horizontal). Three unit cells are shown to illustrate intercalation of anisole species between layers of the porphyrin coordination polymers.

pattern involves an antiparallel arrangement, at close proximity, of the cyanophenyl fragments of adjacent units (the perpendicular distance between the antiparallel Ar−CN axes is about 3.9 Å; Table 3). It is also characterized by the formation of relatively short and nearly linear C−H···N≡C− contacts along the chain (Table 3). Such dimeric aggregation at each site resembles well-known synthons of this type previously observed in numerous other systems.[3,4] In view of the square-planar symmetry of the porphyrin building blocks, this aggregation mode extends in the present structure in two dimensions (along the $a + b$ and c lattice translations), yielding a symmetrically shaped two-dimensional open porphyrin network. It appears to be stabilized by effective dipolar van der Waals interactions assisted by weak hydrogen bonding (see below). The significance of these interactions should be particularly appreciated in the light of relatively close approaches of the negative ends of neighboring CN dipoles (at N···N distances of 3.75 and 3.77 Å) in the observed arrangement (Figure 4a). The interporphyrin voids are conveniently accommodated by two molecules of the chloroform solvent. The planar porphyrin−chloroform layers shown in Figure 4a are stacked in the crystal one on top of the other, in an offset manner, at an average distance of 3.78 Å (Table 3).

Interaction of Zn−TCNPP with ethyl benzoate in the crystallization mixture yields a five-coordinate porphyrin complex (**5**), with the ligand occupying the axial coordination site and thus preventing direct interporphyrin coordination. Therefore, the organization of the porphyrin units is driven primarily, as in the previous example, by dipolar interactions between the cyanophenyl arms along the $a - b$ and c directions of the crystal (Figure 4b). In this case, however, the linear chain motifs of dipolarly linked porphyrins assemble in a second dimension in a slightly different manner, avoiding proximity of similarly oriented dipoles. This yields larger interporphyrin cavities capable of accommodating two ethyl benzoate molecules, one of which is coordinated to the porphyrin core of an adjacent layer while the other fills the remaining interporphyrin space. The interporphyrin pores in **5** are characterized by an approximate 4-fold symmetry as opposed to 2-fold symmetry in **4**. As in other five-coordinate metalloporphyrin structures, the zinc ion deviates (by 0.26 Å) from the planar porphyrin core, toward the bound ligand, assuming a square-pyramidal coordination geometry. In the stacked arrangement of the porphyrin layers, the metal-ligating species protrude into the interporphyrin space of the neighboring and centrosymmetrically related layer. The average distance between the layered porphyrin networks is 4.4 Å, with a somewhat closer porphyrin center-to-porphyrin center approach between the convex surfaces of neighboring layers (4.25 Å) than between the concave ones (4.60 Å). The approximate dimensions of the pores within the two-dimensional porphyrin assemblies available for guest inclusion (after substracting the van der Waals radii of atoms which line the walls of the cavity) are 6.4 × 11 Å in **4** (elliptical shape) and 10 × 10 Å in **5** (nearly square shape).

Layered Triclinic Structures Consisting of Porphyrin Chains. Crystallization of zinc−TCNPP from pure anisole or guaiacol solvents led to the respective formation of compounds **6** and **7**, which represent typical six-coordinated complexes of the metalloporphyrin entity. In **6**, the axial coordination sites are occupied, through $\pi-\pi$ interactions, by two anisole ligands which overlap, and lie nearly parallel to, the porphyrin core from both sides at an average distance of 3.37 Å. The dihedral angle between the planes of the porphyrin core and the overlapping aryl ligand is 11.0°. In **7**, the guaiacol molecules axially coordinate to the zinc center through their hydroxyl groups. The geometry of the zinc coordination is a typically distorted octahedron with equatorial Zn···N(pyrrole) and axial Zn···OH(guaiacol) distances of 2.034(2)−2.047(2) and 2.581(3) Å, respectively. The guaiacol molecular framework is inclined with respect to the porphyrin core by about 30.3°. As shown in Figure 5, the two structures also reveal a layered organization of the 1:2 porphyrin−ligand complexes. The typical, dipolar-stabilized chain organization of the porphyrins prevails, however, only in one direction, but it is disrupted along the other axis. The three-dimensional packing of the layered motifs in these two structures is characterized by an interpenetration of the axial ligand of one layer into the open interporphyrin voids of adjacent layers located above and below (at about 4.1 Å) in order to optimize the interlayer stacking. The need to accommodate the two face-on oriented ligands in any given porphyrin layer requires a relatively large space, thus preventing a close approach between the porphyrin chains and formation of a compact two-dimensional networks as in the previous examples (**4** and **5**). In **7**, the two guaiacol moieties within a given interporphyrin site are weakly hydrogen-bonded to each other around the centers of inversion at OH···O = 3.13 Å. In each layer of the two structures, additional molecules of the corresponding solvent are incorporated into the lattice in a

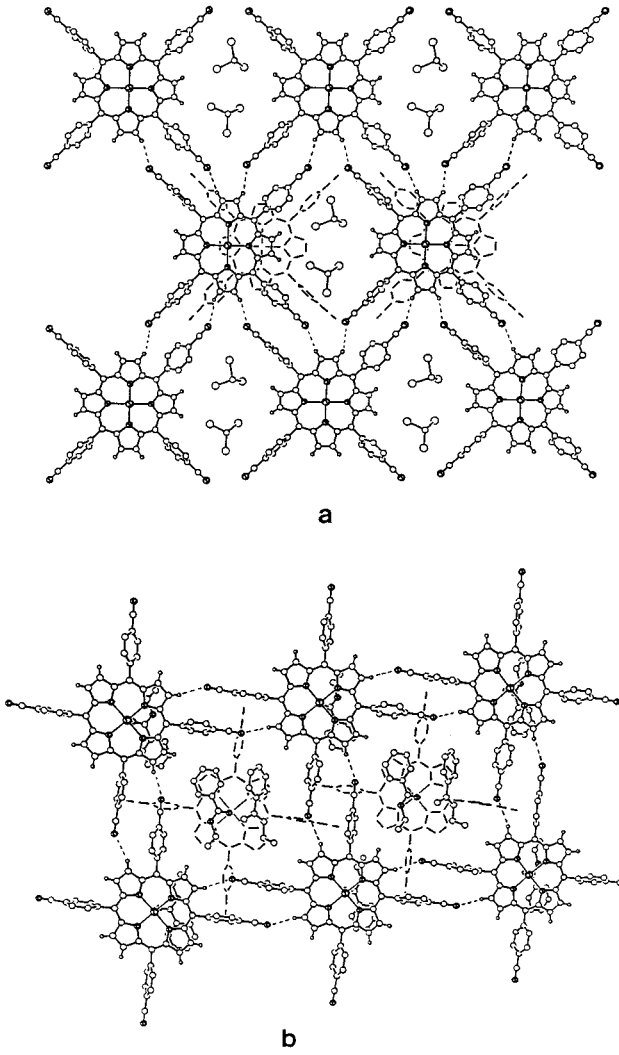

Figure 4. Assembly of the TCNPP building blocks in **4** (a) and **5** (b) in the form of two-dimensional open networks stabilized by dipolar interactions between the PhCN dipoles as well as by weak C−H···N≡C hydrogen bonds (dotted lines). The oval-shaped interporphyrin cavities in **4** are occupied by two molecules of chloroform (a). The square-shaped larger cavities in **5** accommodate two molecules of ethyl benzoate (b). One molecule of ethyl benzoate (with crossed circles marking its O atoms) is ligating to the metal center of a porphyrin unit in adjacent layer. The stick-only frameworks showed in these drawings (as well as in the following ones) illustrate porphyrin molecules in neighboring layers and indicate the layered nature of the crystal structures in **4** and **5**.

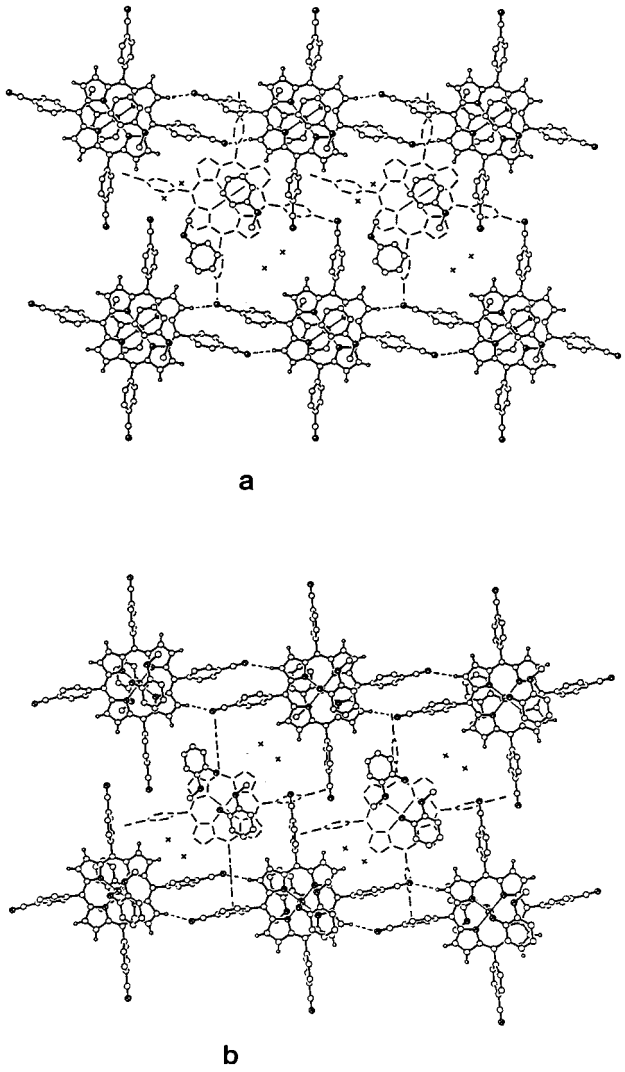

Figure 5. Illustration of the offset-stacked layered architectures in **6** (a) and **7** (b). In these two structures, close interporphyrin association is maintained in only one direction. The layered arrangement is expanded in the other direction in order to accommodate two guest molecules of anisole (in **6**) and guaiacol (in **7**), while preserving a short interlayer spacing of about 4.1 Å. The two guest components are weakly coordinated to the porphyrin units of adjacent layers approaching from above and below (Table 2). Cross signs indicate the approximate positions of additional molecules of noncoordinated disordered solvent within the layers.

disordered manner to fill the remaining empty space between adjacent porphyrin-chain motifs (Figure 5).

A similar porphyrin−solvent composition and intermolecular architecture characterize the crystals of zinc−TNO_2PP with eugenol (**8**). The basic molecular entity in this structure is a six-coordinate complex of the metalloporphyrin with eugenol, the latter occupying two axial coordination sites of the zinc ion at Zn···OH(eugenol) of 2.519(7) Å. Although there are two crystallographically independent porphyrin entities in the asymmetric unit, they deviate from coplanarity by only 3.5°, and this crystal structure is also characterized by a layered arrangement (Figure 6). In each such layer, there are parallel chain motifs of strongly interlinked porphyrin units (Table 3) which are interspaced by eugenol molecules coordinated to the metal centers of neighboring porphyrin sheets. A third noncoordinating eugenol species is also included between these chains. The interlayer spacing is 4.19 Å. Presence of the nitro-substituents on the TPP core, and their nearly perpendicular alignment with respect to the porphyrin core framework, allows for hydrogen bonding interactions between the stacked layered assemblies as well, thus forming "cascaded" networks in which the porphyrin chains in one layer are linked to the porphyrin chains in adjacent layers located above and below (Figure 6). The corresponding interlayer NO_2···HC(pyrrole) H-bonding distances are within the range 3.4−3.5 Å.

Herring-Bone-Type Arrangements of Porphyrin Chains in Monoclinic Structures. Figure 7 shows the intermolecular organization in compounds **9** and **10** and represents "herring-bone"-type clathrates of the four-coordinate TCNPP entity. This type of arrangement was previously observed only in a very small number of monoclinic TPP lattice clathrates.[5] Somewhat surprisingly, crystallization of Zn−TCNPP from a 1:1 mixture of benzene and chloroform did not yield a coordination polymer. However, as in the previously described examples, the basic motif in these two structures remains the linear chain assembly

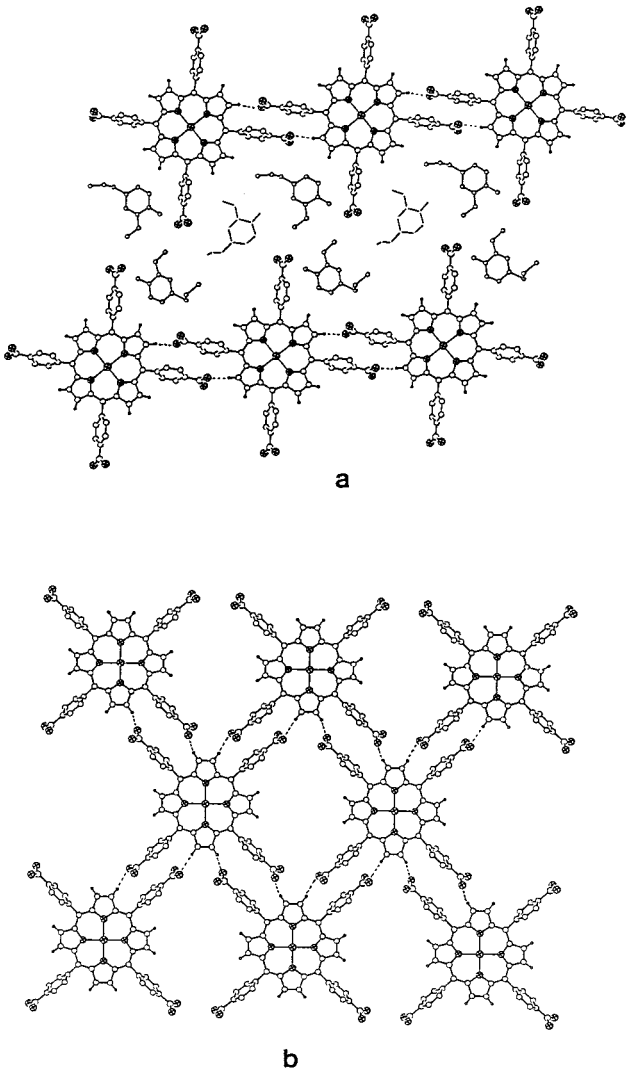

Figure 6. Intermolecular organization in the crystals of zinc−TNO_2-PP with eugenol (**8**). (a) Composition of a single layer in this structure involves linear chains of interlinked porphyrin moieties which are interspaced by the eugenol species. Eugenols represented by ball-and-stick frameworks are coordinated to the overlapping adjacent layers from above and below; those of stick-only type are not coordinated to the porphyrin lattice. (b) Interlayer as well as intralayer hydrogen bonding between the TNO_2PP building blocks in **8**.

of the porphyrin units (along $a + c$) involving the cyclic $(ArCN)_2$ synthon (Table 3). Adjacent chains related by glide-plane symmetry in **9** form once again a porous layered porphyrin arrangement with an interlayer spacing of about 4.3 Å. The intermolecular voids are occupied by molecules of the benzene and chloroform solvents (Figure 7a). The observed arrangement, revealing close C−H(chloroform)···N≡C interaction (CH···NC = 3.32 Å), suggests that partial solvation of the cyano groups by chloroform in the benzene-diluted chloroform solvent could affect the self-coordination ability of the porphyrins. Compound **10**, which was obtained by crystallization of Cu−TCNPP from pure nitrobenzene consists also of similar porphyrin chains extending along the $a + 2c$ direction and reveals the common intermolecular synthon. It provides the only available example of a nonlayered arrangement of the TCNPP frameworks in this study. Adjacent chains in the crystal structure are nearly perpendicular to one another, being cross-linked by secondary hydrogen-bonding-type interactions (Figure 7b). The space between adjacent porphyrin chains is occupied by molecules of the nitrobenzene solvate. The centrosymmetric environment around the metalloporphyrin fragment contributes to the preservation of its planarity in this structure. Molecules of nitrobenzene approach the central porphyrin core from both sides but are not coordinated to the metal ion (shortest Cu···O distances are 3.43 Å) owing to the preference of Cu(II) to maintain a square-planar coordination environment.

The structural data related to the interporphyrin interaction in the layered materials **4**−**9** are summarized in Table 3. Of further particular attention is the translational displacement between adjacent chains of the porphyrin units within the layered zones. Its variation in these solids throws light on the organizational flexibility in crystals of the title compounds and on the nature of the interporphyrin pore structure. In the network arrangements (in **4** and **5**, Figure 4) the two modes of interporphyrin assembly have cavities of different size characterized by chain displacements of about 15.5 Å (in **4**) and 17.5 Å (in **5**). These distances are increased to nearly 20.0 Å (in **6** and **7**) and 23.3 Å (in **8**) to accommodate three guest species within the layers. Finally, in structure **9** the interchain displacement is decreased to 15.0 Å to effectively entrap two small guest molecules of different polarity and lipophilicity in small separated cavities.

Discussion

The characteristic modes of intermolecular architecture in crystalline solids of tetraphenylmetalloporphyrins[5,15] provide an excellent basis for a controlled variation of the supramolecular architectures in these materials. They are well represented by the layered structures of triclinic zinc−TPP and tetragonal zinc−TPP hydrate shown in Figure 8.[15] In each layer (in the present discussion the "layers" are considered to be parallel to the porphyrin plane) the interaction between the phenyl groups of adjacent porphyrin molecules is similar to that observed in solid benzene and other structures containing aryl derivatives.[6] Stacking of these porphyrin layers one on top of the other at regular intervals (e.g., 4.15 Å in the triclinic form and 4.86 Å in the tetragonal form) and in the typical offset manner[6e] forms the third dimension of each lattice. In the numerous clathrates of TPP, the interporphyrin voids between the concave surfaces of adjacent molecules within the layers (which are already evident in the crystal structure of the triclinic zinc−TPP)[15a] are expanded and accommodated by a guest component, while maintaining the distance between the mixed host−guest layers within 4−5 Å.[5] Only a very small number of compounds, out the few hundreds crystallographically analyzed thus far, yield a "herring-bone" organization.[5a] It is thus evident from the large database of such structures that an offset layered arrangement of the roughly flat porphyrin species at a narrow distance range (4−5 Å) is a fundamental property of the porphyrin−porphyrin interaction required to optimize van der Waals stabilization in these solids. It is also apparent that lack of specific intralayer interactions between the porphyrin building blocks allows for little constrained expansion of the porphyrin arrays by inclusion of guest components of versatile size and shape, giving rise to poorly selective formation of "sponge" clathrates.[5]

A number of crystal engineering concepts can be employed to these metallomacrocyclic systems in order to induce more specific mutual recognition (other than through molecular shape) and direct the interporphyrin organization. We have focused in recent years on functionalization of the tetraphenyl periphery

(15) (a) Scheidt, W. R.; Mondal, J. U.; Eigenbrot, C. W.; Adler, A.; Radanovich, L. J.; Hoard, J. L. *Inorg. Chem.* **1986**, *25*, 795−799. (b) Glick, M. D.; Cohen, G. H.; Hoard, J. L. *J. Am. Chem. Soc.* **1967**, *89*, 1996−1998.

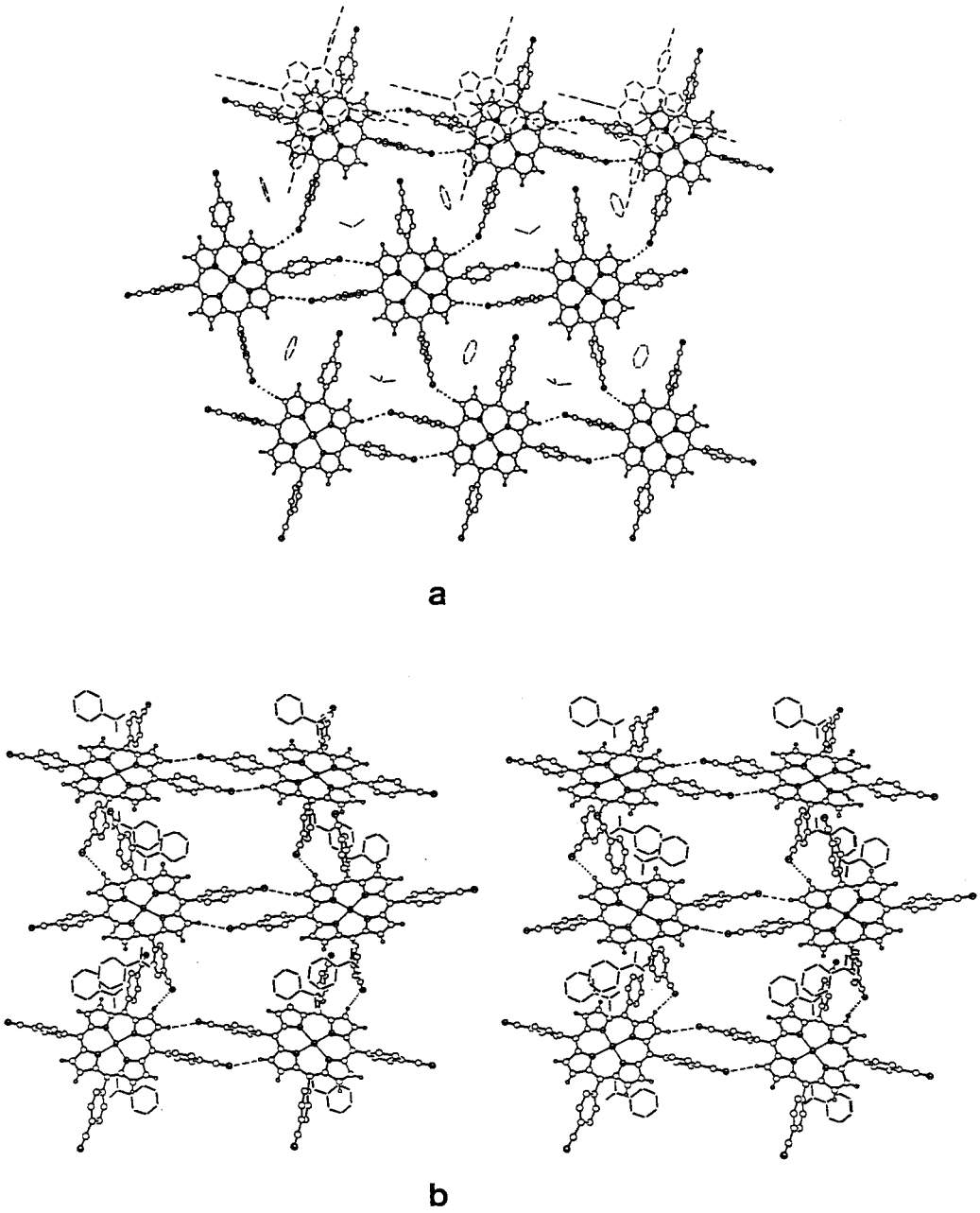

Figure 7. Preservation of the interporphyrin chain organization of TCNPP, propagated by the cyclic $(ArCN)_2$ synthon, in the monoclinic structures **9** (a) and **10** (b). A layered crystalline architecture (with interlayer spacing of 4.3 Å) is still maintained in **9**, with the benzene and chloroform guest components accommodated within the planes of the individual layers. The stereographic projection in (b) illustrates the more rare[5] herring-bone interporphyrin organization in **10**; the nitrobenzene guest species occupy in this structure the concave surfaces formed between adjacent porphyrin chains.

of TPP by adding polar sensor groups, and most successful results have been obtained thus far by a symmetric substitution at the 4-position of the four aryl rings. The results of the present study on the TCNPP system provide an excellent perspective on the preferred modes of supramolecular assembly of porphyrin derivatives with aprotic polar functions. Thus, absence of solvents which can act as axial ligands to the metalloporphyrin core allows for the formation of coordination polymers with diverse dimensionality. Our findings in this study related to the formation of two-dimensional polymeric architectures with TCNPP add to earlier results on multidimensional coordination polymerization based on the TPyPP building blocks,[9g] as well as to few reports by others on dimers, oligomers, and one-dimensional polymers of closely related porphyrinic systems.[8] Formation of the polymeric arrays in the present case is limited to crystallization solvents which can intercalate effectively between the corrugated surfaces of neighboring polymeric layers (Figures 2 and 3).

Presence of competing axial ligands or strongly solvating species in the crystallization environment may prevent self-coordination of the porphyrin building blocks through PhCN-to-metal interaction. In such cases the molecular shape features of the porphyrin materials dictate in most cases the formation of layered structures consisting of flat and *hollow* multiporphyrin assemblies. The porphyrin units within these arrays are interlinked by dipolar forces assisted by C−H···N hydrogen bonding either in one or two dimensions (Figures 5 and 4, respectively). The interlayer separation is typically maintained within the 3.8−4.4 Å range (Table 3), irrespective of the degree of coordination around the metal centers (in lattices based on

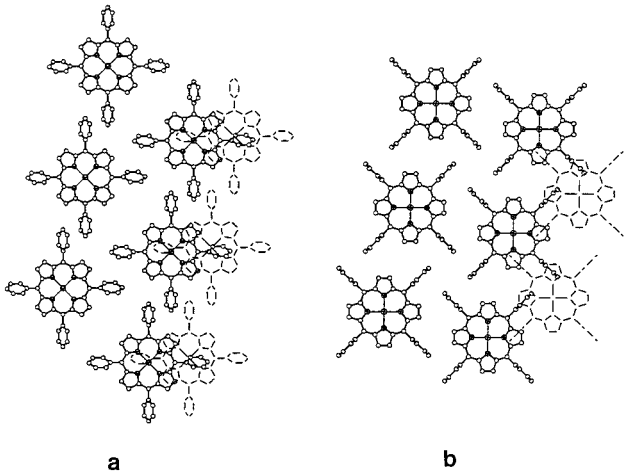

Figure 8. Illustration of the crystal structures of (a) triclinic zinc−TPP[15a] and (b) tetragonal zinc−TPP hydrate,[15b] which exemplify the preferred layered organization of the TPP building blocks in crystals. Similar patterns have been observed in crystals of numerous TPP clathrates.[5] This conservation of the porphyrin structure provides an excellent basis for a controlled variation of supramolecular architectures in these materials by molecular recognition effects.

five-coordinate or six-coordinate entities the axial ligands of one layer are effectively inserted into the interporphyrin pores of adjacent layers), which reflects the significant stabilization associated with such an organization. The conservation of the open porphyrin chain or network motifs and of the interporphyrin offset stacking geometry allows one to control to a considerable extent the porosity of the porphyrin layers by changing the type of the sensor groups attached to the porphyrin framework. Indeed, it has been demonstrated previously that the cavity size characteristics in layered multiporphyrin motifs are significantly different in structures based on the PhOH, PhF, PhCl, or PhBr porphyrin derivatives.[9b] The corresponding van der Waals width of the open space within the multiporphyrin chains ranges from 3.5 Å in the PhOH material (suitable to accommodate an aromatic moiety edge-on) to 5.5 Å in the PhBr material (which can be occupied either by a flattened aryl moiety or by two molecules of a smaller guest as DMSO). The interporphyrin pore size in the layered TCNPP compounds described above is even larger (about 6.4 Å in **4** and 10 Å in **5**), allowing inclusion within these open networks of two $CHCl_3$ units or two larger aryl entities, respectively (Figure 4).

The robustness of the cyclic $(ArCN)_2$ synthon (Figure 9a) is well demonstrated in structures **4**−**7**, **9**, and **10**. It should be attributed to two different aspects of this intermolecular interaction. A rough estimate of the nonbonding interaction energy[16] associated with such a bimolecular arrangement in these structures shows an energy gain in the range 5.3−8.5 kcal/mol, which explains the relative stability of the chain and network motifs in these compounds. The lower range (5.30−5.90 kcal/mol) was obtained for the centrosymmetric patterns of antiparallel cyanophenyl arms in **6** and **7**, while the higher stabilization range of 6.43−8.50 kcal/mol in the other structures relates to a noncentrosymmetric organization of the PhCN pairs (with an additional component of edge-to-face Ph···Ph interaction). Moreover, the nitrogen site is an excellent proton acceptor in

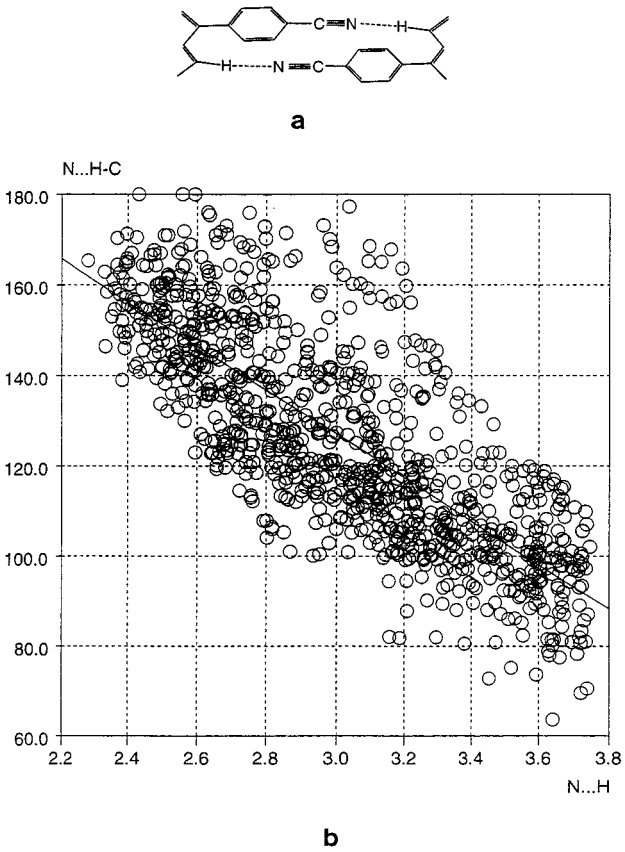

Figure 9. (a) Cyclic $(ArCN)_2$ synthon for intermolecular association discussed in this study. (b) Scattergram of −C≡N···H−C(conjugated) hydrogen bonds found in the literature, which correlates between the N···H distance and the N···H−C angle. This scattergram is based on about 980 entries retrieved from the October 1996 version of the Cambridge Crystallographic Database.[3]

hydrogen bonding even with weak acids, as it is illustrated in thousands of examples reported in the literature.[3,11] Figure 9b shows a scattergram of −C≡N···H−C(conjugated) hydrogen bonds which is based on about 980 entries retrieved from the October 1996 version of the Cambridge Crystallographic Database.[3] It clearly indicates that shorter bonds (H···N ≤ ∼2.6 Å), which obviously reflect on stronger attraction, are typicaly associated with a near-linear (≥140°) N···H−C arrangement. Current observations in the layered structures **4**−**7**, **9**, and **10** fall in the same category (Table 3), suggesting a significant contribution of the −C≡N···H−C interaction to the stabilization of the TCNPP chain and network patterns.

Concluding Remarks

The present series of studies on the self-assembly of functionalized metalloporphyrins[9] is an important step toward the design of coordination polymers and noncovalent synthesis of porous organic solids. It demonstrates the feasibility, by rational modification of the porphyrin building blocks with protic or aprotic polar sensor groups, of a controlled formulation of supramolecular multiporphyrin arrays *via* coordination, hydrogen bonding and dipolar attraction. The molecular recognition features inherent to the introduced functionality add an important element of selectivity into the formed porphyrin lattice. As opposed to the "sponge" character of the simple porphyrin-based clathrates, which are relatively insensitive to the nature and size of the guest species (see above),[5] the layered functionalized materials are characterized by a better defined pore structure

(16) The van der Waals stabilization energies were estimated by semiempirical computational methods using the Biosym software (Biosym Technologies, San Diego, CA 1994) and standard atom−atom potentials. See also: Hagler, A. T.; Dauber, P.; Lifson, S. *J. Am. Chem. Soc.* **1979**, *101*, 5131−5141.

and are, thus, more selective toward potential guest components within the interporphyrin voids. Further studies are currently under way to explore on a more quantitative basis the selectivity features of the porphyrin-based crystalline networks and their potential in molecular transport and guest release applications. Designed supramolecular syntheses of additional systems are also in progress.[17] The porphyrin metallomacrocycles provide an outstanding example of molecular building blocks, the self-organization of which is largely affected by molecular shape. Correspondingly, their predictable crystalline architectures can be readily fine-tuned in a systematic manner by common "tools" of molecular recognition.[4,18]

(17) Preliminary results show successful supramolecular syntheses of hydrogen-bonded crystalline polymers based on tetrakis(4-amidophenyl)porphyrin, and of metal-chelated polymers of 4-*N*-acetoacetamidophenylporphyrin.

Acknowledgment. This work was supported in part by the Israel Science Foundation administered by the Israel Academy of Sciences and Humanities and by Grant No. 94-00344 from the United States−Israel Binational Science Foundation (BSF), Jerusalem, Israel.

Supporting Information Available: X-ray crystallographic data for the ten compounds listed in Table 1, including tables of atomic coordinates (before and after the "Squeeze" procedure[14] for the relevant structures), temperature factors, bond distances and angles (62 pages). An X-ray crystallographic file for compounds **1**−**10**, in CIF format, is available on the Internet. See any current masthead page for ordering and Internet access instructions.

IC971259U

(18) Wolff, J. J. *Angew. Chem., Int. Ed. Engl.* **1996**, *35*, 2195−2197.